ACS APPLIED MATERIALS & INTERFACES

Letter

www.acsami.org

Au-Nanoparticle-Loaded Graphitic Carbon Nitride Nanosheets: Green Photocatalytic Synthesis and Application toward the Degradation of Organic Pollutants

Ningyan Cheng,[†,‡] Jingqi Tian,[†,‡] Qian Liu,[†] Chenjiao Ge,[†] Abdullah H. Qusti,[§,⊥] Abdullah M. Asiri,[§,⊥] Abdulrahman O. Al-Youbi,[§,⊥] and Xuping Sun*[,†,§,⊥]

[†]State Key Lab of Electroanalytical Chemistry, Changchun Institute of Applied Chemistry, Chinese Academy of Sciences, Changchun 130022, Jilin, China

[‡]Graduate School of the Chinese Academy of Sciences, Beijing 100039, China

[§]Chemistry Department, Faculty of Science, and [⊥]Center of Excellence for Advanced Materials Research, King Abdulaziz University, Jeddah 21589, Saudi Arabia

ABSTRACT: Au nanoparticles (AuNPs) were loaded on graphitic carbon nitride (g-C_3N_4) nanosheets prepared by ultrasonication-assisted liquid exfoliation of bulk g-C_3N_4 via green photoreduction of Au(III) under visible light irradiation using g-C_3N_4 as an effective photocatalyst. The nanohybrids show superior photocatalytic activities for the decomposition of methyl orange under visible-light irradiation to bulk g-C_3N_4, g-C_3N_4 nanosheets, and AuNP/bulk g-C_3N_4 hybrids.

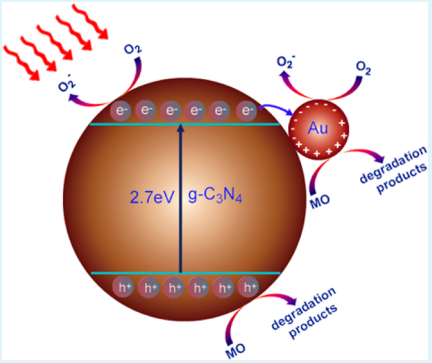

KEYWORDS: *graphitic carbon nitride, nanosheets, Au nanoparticles, green synthesis, photodegradation, methyl orange*

INTRODUCTION

Modern commercial dyes are characterized by strong structural and color stability due to their high degree of aromaticity and extensively conjugated chromophores. Synthetic dyes are extensively used in many fields and their unintended release into the environment poses potential risk to human health and ecological systems.[1] Thus, effective removal of synthetic dyes from wastewater is highly important. Activated carbon can effectively adsorb the dye in water,[2] but it suffers from expensive price. Photocatalysis using semiconductors enables pollutant decomposition and has received considerable attention during the past decades. TiO_2 is considered as one of the best photocatalysts, but it can absorb only the UV portion of the solar spectrum because of its wide bandgap of 3.2 eV.[3,4] Such issue can be solved by using narrow bandgap semiconductors adsorbing visible light, such as CdS,[5] $BiVO_4$,[6] Bi_2WO_6,[7] etc.

Recent years have witnessed the wide application of carbon materials with graphite-like structures, such as graphene and boron carbonitride (BCN).[8−11] As an analogue of graphite, graphitic carbon nitride (g-C_3N_4) polymer with bandgap of 2.7 eV is the most stable allotrope of carbon nitride possessing a stacked two-dimensional structure under ambient conditions.[12] Compared with inorganic semiconductor counterparts, g-C_3N_4 is a sustainable and environmentally friendly organic semiconductor that consists of carbon and nitrogen, which are among the most abundant elements in our planet. Since its photocatalytic performance was reported by Wang et al.,[13] g-C_3N_4 has found intensive applications in the photocatalytic and photovoltaic fields.[14,15] In general, catalytic activity of a catalyst can be improved by increasing its specific surface area (SSA).[16] Sano et al. reported that photocatalytic activity of g-C_3N_4 toward NO oxidation in gas phase can be significantly improved by increasing its surface area via alkaline hydrothermal treatment.[17] Chen et al. reported that mesoporous Fe-g-C_3N_4 shows improved photocatalytic performances for the direct oxidation of benzene to phenol than bulk conterpart.[18] It is thus rational to conclude that increasing SSA of g-C_3N_4 can effectively improve the photocatalytic degradation rate of dyes. On the other hand, given that gold nanoparticles (AuNPs) can serve as photocatalysts for the degradation of dyes under visible-light irradiation,[19] it is expected that the photocatalytic performances of g-C_3N_4 can be further improved after loading of AuNPs.

As a two-dimensional nanostructure, g-C_3N_4 nanosheets should exhibit superior physicochemical properties, such as

Received: May 13, 2013
Accepted: July 12, 2013
Published: July 12, 2013

   dx.doi.org/10.1021/am401802r | *ACS Appl. Mater. Interfaces* 2013, 5, 6815−6819

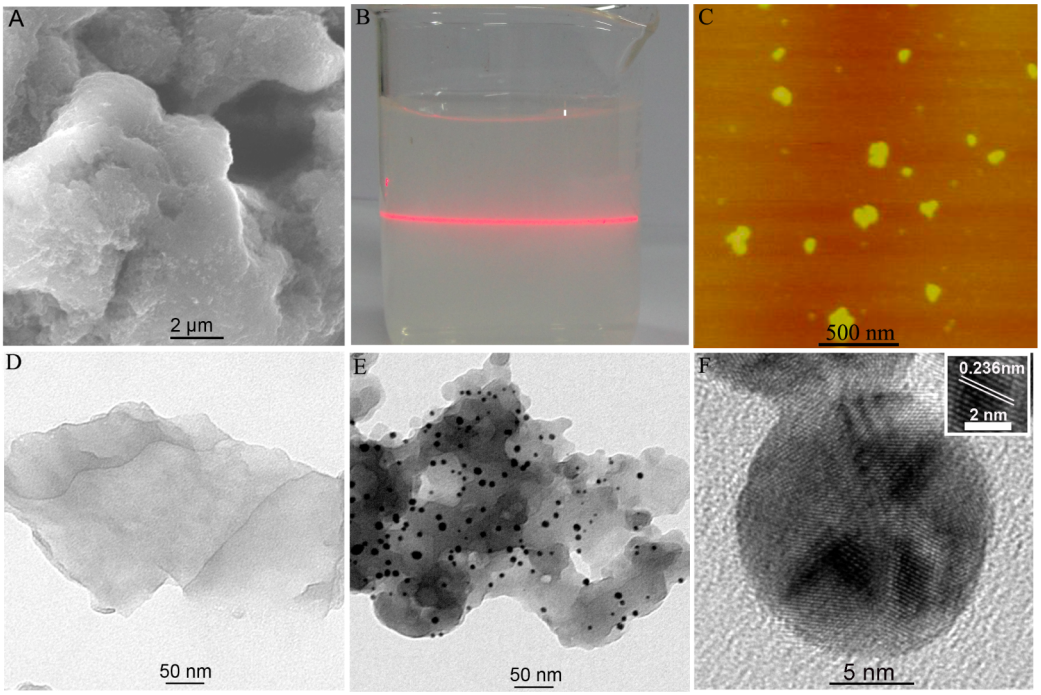

Figure 1. (A) SEM image of bulk g-C_3N_4, (B) Tyndall effect exhibited by aqueous dispersion of g-C_3N_4 nanosheets passed through with red laser light, (C) AFM and (D) (TEM) images of g-C_3N_4 nanosheets, (E) TEM image of AuNP/g-C_3N_4 nanohybrids, and (F) high-magnification TEM image and corresponding HRTEM image (inset) of one single AuNP.

larger surface area and shorter photoinduced charger carriers transferring distance, than bulk g-C_3N_4. However, to the best of our knowledge, the use of g-C_3N_4 nanosheets as a photocatalyst has never been reported before. In this paper, for the first time, g-C_3N_4 nanosheets were used as a support and photocatalyst for the green synthesis of AuNPs loaded g-C_3N_4 nanosheets (AuNP/g-C_3N_4). It suggests that the resulting nanohybrids show greatly enhanced catalytic activities to the visible-light decomposition of methyl orange (MO) than bulk g-C_3N_4, g-C_3N_4 nanosheets, and AuNP/bulk g-C_3N_4 hybrids.

EXPERIMENTAL SECTION

Materials. Melamine, chloroauric acid, and MO were purchased from Aladdin Ltd. (Shanghai, China). All chemicals were used as received without further purification. The water used throughout all experiments was purified through a Millipore system.

Preparation of g-C_3N_4 Nanosheets. The bulk was prepared by polymerization of melamine molecules under high temperature. In detail, melamine was heated at 600 °C for 2 h under air condition with a ramp rate of about 3 °C/min for the heating process. The obtained yellow products were bulk g-C_3N_4. g-C_3N_4 nanosheets were prepared by exfoliation of as-prepared bulk g-C_3N_4 in water. In brief, 0.1 g of bulk g-C_3N_4 power was dispersed in 200 mL of water, and the mixture was ultrasound for 16 h.[20,21] The resulting suspension was centrifuged at 5000 rpm to remove the residual unexfoliated g-C_3N_4, followed by centrifugation at 15000 rpm to obtain g-C_3N_4 nanosheets. The yield of the g-C_3N_4 nanosheets is calculated to be about 8.6%. The products were dried in air and then redispersed in water for characterization and further use.

Preparation of AuNP/g-C_3N_4 Nanohybrids. Sixty milligrams of as-prepared g-C_3N_4 nanosheets was dispersed in 42 mL of $HAuCl_4$ (0.055 mM) aqueous solution. The mixture was stirred in the dark for 1 h, followed by adding 8 mL of methanol. The mixture was degassed under nitrogen for 10 min and stirred under visible light for 1 h in the ice water bath. After that, it was centrifuged at 15 000 rpm. The products were dried in air and then redispersed in water for characterization and further use. The AuNP/bulk g-C_3N_4 was prepared using the same method.

Photocatalytic Activity. The photocatalytic activities of the samples were evaluated by the photocatalytic degradation of methyl orange in an aqueous solution under visible light irradiation. A500W Xe lamp with a 400 nm cutoff filter was used as the light source to provide visible irradiation. In the experiment, 45 mg of photocatalyst was added into 15 mL of methyl orange solution with a concentration of 10 mg/L. Prior to irradiation, the suspensions were magnetically stirred in the dark for 30 min to obtain the saturated absorption of methyl orange onto the catalysts. At irradiation time intervals of every 0.5 h, the suspensions were collected and then centrifuged (15 000 rpm, 10 min) to remove the phtocatalyst particles. The concentrations of the methyl orange were monitored using a UV−vis spectrophotometer during the photodegradation process.

Characterizations. Scanning electron microscopy (SEM) measurements were made on a XL30 ESEM FEG scanning electron microscope at an accelerating voltage of 20 kV. Transmission electron microscopy (TEM) measurements were made on a Hitachi H-8100 EM (Hitachi, Tokyo, Japan) with an accelerating applied potential of 200 kV. The UV−vis spectra were recorded on a UV580C spectrophotometer. Powder X-ray diffraction (XRD) data were recorded on a RigakuD/MAX 2550 diffractometer with Cu Kα radiation (λ = 1.5418 Å). The Brunauer−Emmett−Teller (BET) surface area and pore volume were measured on a Quantachrome NOVA 1000 system at liquid N_2 temperature. For photodegradation a 500 W xenon lamp (CHFXQ500W, Beijing) with cutoff filter (λ > 400 nm) was used.

dx.doi.org/10.1021/am401802r | ACS Appl. Mater. Interfaces 2013, 5, 6815−6819

RESULTS AND DISCUSSION

Figure 1A shows the SEM image of the bulk g-C_3N_4, indicating they are solid agglomerates about several micrometers in size. The occurrence of the Tyndall effect of the diluted aqueous dispersion of the products obtained after ultrasolication treatment of bulk g-C_3N_4 (Figure 1B) reveals the colloidal nature of the dispersion. Figure 1C presents the AFM image of the resulting colloidal particles, indicating that they are nanosheets well separated from each other. Figure 1D presents the TEM image of the g-C_3N_4 nanosheets. All these observations suggest the successful exfoliation of bulk g-C_3N_4 into nanosheets. After visible-light irradiation of the nanosheets in the presence of Au(III) salt, a large amount of nanoparticles with diameters in the range 5−20 nm are generated on the nanosheets, as shown in Figure 1E. Figure 1F shows the high-magnification TEM image of one single nanoparticle, indicating it is spherical in shape. The high-resolution TEM (HRTEM) image taken from the nanoparticle (inset) reveals clear lattic fringes with an interplane distance of 0.236 nm corresponding to the (111) lattice space of metallic Au,[22] indicating the nanoparticle is AuNP. All these observations show the formation of AuNP-loaded g-C_3N_4 nanosheets.

Figure 2 shows the XRD patterns of bulk g-C_3N_4, g-C_3N_4 nanosheets, and AuNP/g-C_3N_4 nanohybrids. Bulk g-C_3N_4

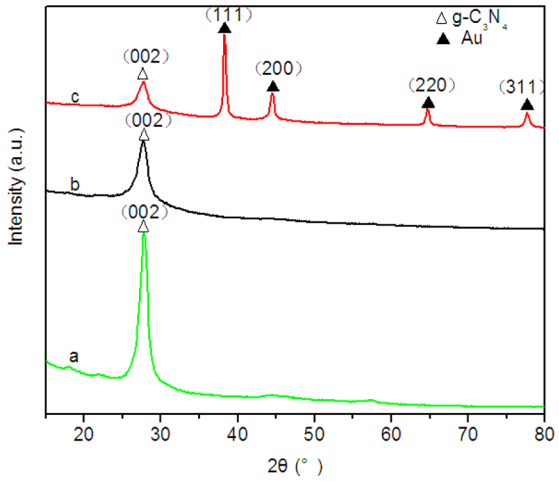

Figure 2. XRD patterns of (a) bulk g-C_3N_4, (b) g-C_3N_4 nanosheets, and (c) AuNP/g-C_3N_4 nanohybrids.

(curve a) shows one strong peak located at 27.4° corresponding to the reflection from (002) plane of g-C_3N_4, which is consistent with the standard value (JCPDS 87−1526).[23] In contrast, the g-C_3N_4 nanosheets (curve b) only show much weaker (002) peak, further suggesting the exfoliation of bulk g-C_3N_4 after ultrasonication treatment. Compared with g-C_3N_4 nanosheets, the nanohybrids (curve c) exhibit four additional peaks located at 38.2, 44.4, 64.6, and 77.5° corresponding to 111, 200, 220, and 311 faces of Au, respectively. Such observations provide another piece of evidence to support the formation of AuNPs after irradiation.[24]

Figure 3 shows the UV−vis diffuse reflectance spectra (DRS) of bulk g-C_3N_4, g-C_3N_4 nanosheets and AuNP/g-C_3N_4 nanohybrids. The intrinsic absorption edge of g-C_3N_4 nanosheets (curve a) shows a slight blue shift in comparison with the bulk g-C_3N_4 (curve b). Compared with g-C_3N_4 nanosheets, the AuNP/g-C_3N_4 nanohybrids (cuve c) show an additional absorption peak around 550 nm characteristic of the colloidal

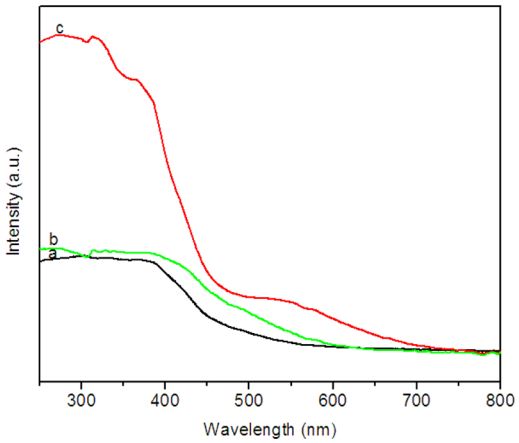

Figure 3. UV−vis diffuse reflectance spectra of (a) g-C_3N_4 nanosheets, (b) bulk g-C_3N_4, and (c) AuNP/g-C_3N_4 nanohybrids.

gold surface plasmon resonance band, further confirming the formation of AuNPs.[13] Besides, the hybrids also show increased absorption in UV region, which can be attributed to the UV-light absorption of AuNPs.[19]

The photocatalytic activities of as-prepared samples were evaluated by the degradation of organic dye under visible-light irradiation. MO as a representative hazardous dye was chosen in our work. To all of the samples, the photodegradation process of MO was recorded by the temporal evolution of the spectrum. Figure 4 shows the photocatalytic activities of the

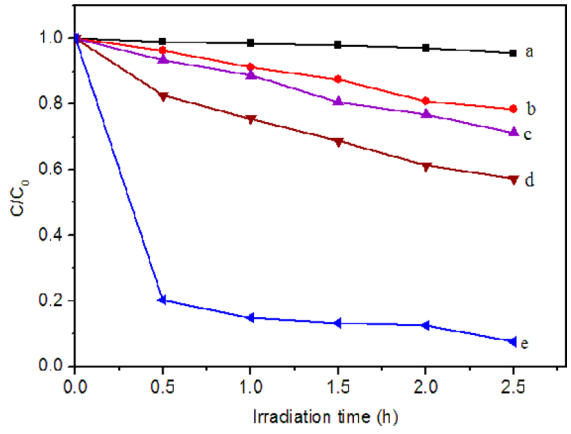

Figure 4. Degradation rate of methyl orange under visible-light irradiation in the presence of (a) blank, (b) bulk g-C_3N_4, (c) g-C_3N_4 nanosheets, (d) AuNP/bulk g-C_3N_4 hybrids, and (e) AuNP/g-C_3N_4 nanohybrids.

samples under visible light irradiation (λ > 400 nm). For comparison, MO photodegradation without photocatalyst was also examined and the results demonstrated that the degradation of MO was very low in the absence of photocatalyst under visible-light irradiation. Only 21.5% MO can be photodegraded by bulk g-C_3N_4 in 150 min. The use of g-C_3N_4 nanosheets leads to 28.7% photodegradation of MO. After loading AuNPs, the AuNP/g-C_3N_4 nanohybrids can photodegade 92.6% MO, whereas the AuNPs/bulk g-C_3N_4 hybrids can only photodegrade 42.4% MO. It suggests that the nanosheets have higher photocatalytic performance than the bulk, which can be attributed to the higher specific surface area of g-C_3N_4 nanosheets. It also suggests that AuNPs can greatly

dx.doi.org/10.1021/am401802r | ACS Appl. Mater. Interfaces 2013, 5, 6815−6819

enhance the catalytic activities of g-C_3N_4. The SSA of the catalysts was measured by adsorption using the BET isotherm. The SSA of g-C_3N_4 nanosheets is 16.2 m^2 g^{-1}, which is about 2 times as high as that of the bulk g-C_3N_4 (7.94 m^2 g^{-1}). After AuNPs loading, the SSA of g-C_3N_4 nanosheets and bulk g-C_3N_4 were increased up to 18.1 and 8.21 m^2 g^{-1}, respectively, which indicates that loading of AuNPs can further increase the SSA of g-C_3N_4. The superior physicochemical properties of g-C_3N_4 nanosheets including larger SSA and shorter photoinduced charger carriers transferring distance attribute to its higher catalytic activity than bulk g-C_3N_4.

The use of g-C_3N_4 for dye photodegradation has been reported by several authors.[25−28] The mechanism of photocatalytic degradation of MO over AuNP/g-C_3N_4 nanohybrids under visible-light irradiation is proposed as follows and the schematic diagram is presented in Scheme 1. Visible -light

Scheme 1. Schematic Diagram Illustrating the Photocatalytic Degradation of MO over AuNP/g-C_3N_4 Nanohybrid under Visible-Light Irradiation

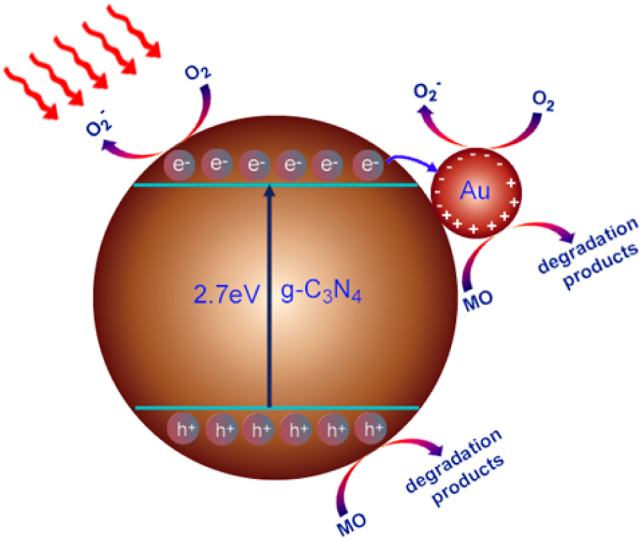

irradiation of g-C_3N_4 nanosheets generates conduction band electrons (e^-) and valence band holes (h^+). The photogenerated electrons could react with O_2 existed in the photodegradation system, reducing it to superoxide radical anion O_2^-. The MO molecules were degradated by the photogenerated h^+ and the O_2^-. The loaded AuNPs could act as electron traps to facilitate the sepration of photogenerated electron−hole pairs and promote interfacial electron transfer process.[25] Furthermore, pasmonic excitation of AuNPs results in the generation of additional electrical surface charges.[29−31] Both these electrons and those transferred from the conduction band of g-C_3N_4 can also react with O_2 to generate O_2^-, providing another pathway to MO degradation. Given the relatively high electronegativity of gold, the AuNPs can capture electrons from the MO molecules adsorbed on them to neutralize the positive charges. As a result, MO oxidization occurs, which is also responsible for the decomposition of MO molecules.

Because renewable catalytic activity is another important factor for a photocatalyst, we further investigated the stability of the AuNP/g-C_3N_4 nanohybrids by a recycling test, as shown in Figure 5. After three cycles, there was no significant loss of activity after being irradiated for 450 min, indicating that the photocatalyst is stable during the photocatalytic test.

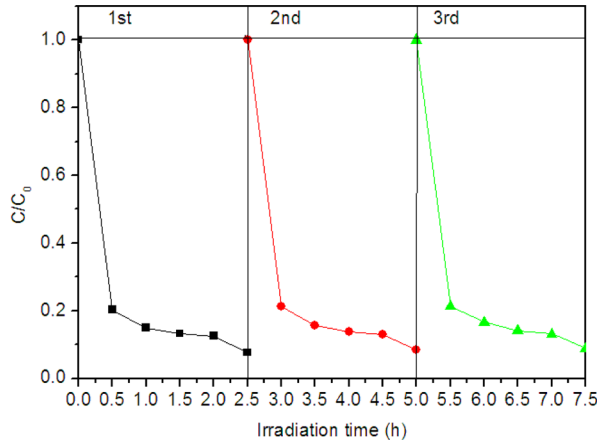

Figure 5. Cycling runs in photocatalytic degradation of MO in the presence of AuNP/g-C_3N_4 nanohybrids under visible light.

CONCLUSION

In summary, visible-light irradation of Au(III) salt in the presence of g-C_3N_4 nanosheets has been proven to be an effective strategy toward green prepration of AuNP/g-C_3N_4 nanohybrids for the first time. The nanohybrids show enhanced photocatalytic performance than bulk g-C_3N_4, g-C_3N_4 nanosheets, and AuNP/bulk g-C_3N_4 hybrids, which can be attributed to the high specific surface area of g-C_3N_4 nanosheets, AuNPs-facilitated sepration of photogenerated electron−hole pairs, and the surface plasmon resonance excitation in AuNPs. Our present study is important for the following two reasons: (1) it is the first demonstration of using g-C_3N_4 nanosheets as an effecient photocatalyst for green synthesis of AuNPs on g-C_3N_4 nanosheets for degradation of organic pollutants; (2) it provides us a new functional material for photovoltaic and photocatalytic applications.[14,15]

AUTHOR INFORMATION

Corresponding Author

*E-mail: sunxp@ciac.jl.cn. Tel/Fax: 0086-431-85262065.

Notes

The authors declare no competing financial interest.

ACKNOWLEDGMENTS

This work was supported by the National Natural Science Foundation of China (21175129), the National Basic Research Program of China (2011CB935800), and the Scientific and Technological Development Plan Project of Jilin Province (20110448).

REFERENCES

(1) Forgacs, E.; Cserháti, T.; Oros, G. *Environ. Int.* **2004**, *30*, 953−971.
(2) Walker, G. M.; Weatheley, L. R. *Water Res.* **1999**, *33*, 1895−1899.
(3) Asahi, R.; Morikawa, T.; Ohwaki, T.; Aoki, K.; Taga, Y. *Science* **2001**, *293*, 269−271.
(4) Ge, L.; Xu, M.; Fang, H.; Su, M. *Appl. Surf. Sci.* **2006**, *253*, 720−725.
(5) Lee, Y. L.; Chi, C. F.; Liau, S. Y. *Chem. Mater.* **2010**, *22*, 922−927.

(6) Kudo, A.; Omori, K.; Kato, H. *J. Am. Chem. Soc.* **1999**, *121*, 11459−11467.
(7) Ren, J.; Wang, W.; Sun, S. *Appl. Catal., B* **2009**, *92*, 50−55.
(8) Wang, X.; Li, X.; Zhang, L.; Yoon, Y. K.; Weber, P. K.; Wang, H.; Guo, J.; Dai, H. *Science* **2009**, *324*, 768−771.
(9) Li, X.; Cai, W.; An, J.; Kim, S.; Nah, J.; Yang, D.; Piner, R.; Velamakanni, A.; Jung, I.; Tutuc, E.; Banerjee, S. K.; Colombo, L.; Ruoff, R. S. *Science* **2009**, *324*, 1312−1314.
(10) Zhang, Y.; Tang, T.; Girit, C.; Hao, Z.; Martin, M. C.; Zettl, A.; Crommie, M. F.; Shen, Y.; Wang, F. *Nature* **2009**, *459*, 820−823.
(11) Liu, A.; Wentzovitch, R. M.; Cohen, M. L. *Phys. Rev. B* **1989**, *39*, 1760−1765.
(12) Groenewolt, M.; Antonietti, M. *Adv. Mater.* **2005**, *17*, 1789−1792.
(13) Wang, X.; Maeda, K.; Thomas, A.; Takanabe, K.; Xin, G.; Carlsson, J. M.; Domen, K.; Antonietti, M. *Nat. Mater.* **2009**, *8*, 76−80.
(14) Niu, P.; Zhang, L.; Liu, G.; Cheng, H. *Adv. Funct. Mater.* **2012**, *22*, 4763−4770.
(15) Wang, X.; Blechert, S.; Antonietti, M. *ACS Catal.* **2012**, *2*, 1596−1606.
(16) Wu, M.; Mu, L.; Wang, Y.; Lin, Y.; Guo, H.; Ma, T. *J. Mater. Chem. A* **2013**, *1*, 7519−7524.
(17) Sano, T.; Tsutsui, S.; Koike, K.; Hiakawa, T.; Teramoto, Y.; Negishi, N.; Takeuchi, K. *J. Mater. Chem. A* **2013**, *1*, 6489−6496.
(18) Chen, X.; Zhang, J.; Fu, X.; Antonietti, M.; Wang, X. *J. Am. Chem. Soc.* **2009**, *131*, 11658−11659.
(19) Zhu, H.; Chen, X.; Zheng, Z.; Ke, X.; Jaatinen, E.; Zhao, J.; Guo, C.; Xie, T.; Wang, D. *Chem. Commun.* **2009**, 7524−7526.
(20) Zhang, X.; Xie, X.; Wang, H.; Zhang, J.; Pan, B.; Xie, Y. *J. Am. Chem. Soc.* **2013**, *135*, 18−21.
(21) Tian, J.; Li, Q.; Asiri, A. M.; Al-Youbi, A. O.; Sun, X. *Anal. Chem.* **2013**, *85*, 5595−5599.
(22) Qin, X.; Lu, W.; Chang, G.; Luo, Y.; Asiri, A. M.; Al-Youbi, A. O.; Sun, X. *Gold Bull.* **2012**, *45*, 61−67.
(23) Ge, L.; Han, C.; Liu, J. *J. Mater. Chem.* **2012**, *22*, 11843−11850.
(24) Sun, X.; Dong, S.; Wang, E. *Angew. Chem., Int. Ed.* **2004**, *43*, 6360−6363.
(25) Ge, L.; Han, C.; Liu, J.; Li, Y. *Appl. Catal., A* **2011**, *409*−*410*, 215−222.
(26) Ge, L.; Han, C.; Liu, J. *Appl. Catal., A* **2011**, *108*−*109*, 100−107.
(27) Yan, S.; Li, Z.; Zou, Z. *Langmuir* **2009**, *25*, 10397−10401.
(28) Yan, S.; Li, Z.; Zou, Z. *Langmuir* **2010**, *26*, 3894−3901.
(29) Li, H.; Liu, S.; Tian, J.; Wang, L.; Lu, W.; Luo, Y.; Asiri, A. M.; Al-Youbi, A. O.; Sun, X. *ChemCatChem* **2012**, *4*, 1079−1083.
(30) Tian, Y.; Tatsuma. *J. Am. Chem. Soc.* **2005**, *127*, 7632−7637.
(31) Yuzawa, Y.; Yoshida, T.; Yoshida, H. *Appl. Catal., B* **2012**, *115*−*116*, 294−302.